LA-6106-MS
Informal Report

UC-79p
Reporting Date: September 1975
Issued: November 1975

Preliminary Topical Report on Comparison Reactor Disassembly Calculations

by

T. P. McLaughlin

los alamos
scientific laboratory
of the University of California
LOS ALAMOS, NEW MEXICO 87545

An Affirmative Action/Equal Opportunity Employer

UNITED STATES
ENERGY RESEARCH AND DEVELOPMENT ADMINISTRATION
CONTRACT W-7405-ENG. 36

In the interest of prompt distribution, this report was not edited by the Technical Information staff.

Work supported by the U. S. Energy Research and Development Administration, Division of Reactor Research and Development, Program No. D554.

Printed in the United States of America. Available from
National Technical Information Service
U S Department of Commerce
5285 Port Royal Road
Springfield, VA 22151
Price: Printed Copy $4.00 Microfiche $2.25

ABSTRACT

This report describes preliminary results of comparison disassembly calculations for a representative LMFBR model (2100-ℓ voided core) and arbitrary accident conditions. The analytical methods employed were the computer programs: FX2-POOL, PAD, and VENUS-II. Calculations were performed at Argonne National Laboratory, Brigham Young University, and Los Alamos Scientific Laboratory. The calculated fission energy depositions are in good agreement, as are measures of the destructive potential of the excursions, kinetic energy, and work. However, in some cases the resulting fuel temperatures are substantially divergent. Differences in the fission energy deposition appear to be attributable to residual inconsistencies in specifying the comparison cases. In contrast, temperature discrepancies probably stem from basic differences in the energy partition models inherent in the codes. Although explanations of the discrepancies are being pursued, the preliminary results indicate that all three computational methods provide a consistent, global characterization of the contrived disassembly accident.

I. INTRODUCTION

The calculation of standard problems by different groups and with different methods is a widely practiced technique for improving understanding of and confidence in various analytical methods. This report describes preliminary results of comparison analyses of hypothetical core disruptive accident conditions. The specific area of interest is that regime of the postulated accident which is analyzed by a disassembly code, e.g., VENUS-II.

The initial impetus for this study was provided by W. R. Stratton of the LASL. Subsequently, a meeting was held in the spring of 1975 to discuss the feasibility and utility of such calculations as well as to specify the ground rules, if accord was reached that such would be practical and beneficial. At that meeting it was decided that the exercise would be worthwhile for (at least) the following reasons.

- Although gross disagreement was not expected, documentation of a comprehensive comparison did not exist.

- Should serious disagreements arise, these would indicate areas where differences in the calculational models are significant and possibly areas where experiments are required.

- Reporting of results of disassembly analyses by various

TABLE OF CONTENTS

groups has, to date, been inconsistent. In particular the kinetic energy or work, as distinct from the thermal (fission) energy release, has apparently led to misconceptions of the measure of severity of the postulated accident.

The individuals (and their organizations) who expressed interest in participating in the actual calculations were:

P. B. Abramson	ANL - AP Div.
C. L. Allen	NRC
J. E. Boudreau	LASL - T-Div
J. F. Jackson	Brigham Young U.
T. P. McLaughlin	LASL - A-Div
D. Weber	ANL - RAS Div.

Due to other work commitments and redundancy in the computer codes being employed, C. L. Allen and D. Weber did not contribute to this first round of intercomparisons.

The applicability of the hydrodynamic models in disassembly codes is in general related to the severity of the postulated excursion. That is, for mild nuclear explosions such as the KIWI-TNT excursion, it has been possible to calculate significant parameters (fission energy, kinetic energy) to within a factor of 2 of the estimated experimental values.[1] On the other hand, postulated LMFBR meltdown accidents, during which material moves but hydrodynamic disassembly does not occur, would not be amenable to analyses by current disassembly codes.

In order to investigate this range of applicability it

was decided to calculate the agreed upon standard problems (based on a 2100-ℓ voided core model) for input reactivity insertion rates of 20, 100, and 200$/s. It should be emphasized that these extreme reactivity insertions were contrived solely for intercomparing calculational methods, and are not based on any calculations concerning particular hypothetical accident scenarios. At this time analyses have been performed only for 100$/s reactivity ramps. Upon completion of this phase of the intercomparison study, calculations will be performed for ramps of 20 and 200$/s.

For intercomparing analytical methods, the consensus of those at the aforementioned organizational meeting was that agreement in total fission energy release within a few tens of percent ($\lesssim$ 30%) would be both expected and desirable. Better agreement would be encouraging; however, considering the many and basic differences in the geometric, hydrodynamic, and neutronic models incorporated into these codes, this was not considered necessary for applications to postulated severe reactor disassemblies. Of course validation of these codes on an absolute scale is also necessary to insure that although they are internally consistent; they are also complete in the modeling of phenomena.

II. ANALYTICAL METHODS

Four computer codes were considered in this first series of calculations. They were:

FX2-POOL

FX2-VENUS

PAD

VENUS-II

The FX2-VENUS analysis was attempted by P. B. Abramson at ANL. This did not prove feasible for the purpose at hand due to difficulties associated with mesh distortion and mapping.

FX2 requires an Eulerian grid and VENUS employs a Lagrangian grid. As grid distortion (i.e., core disassembly) occurs, the FX2-VENUS technique requires remapping of the distorted (VENUS) grid onto the Eulerian (FX2) grid. Although in principle FX2-VENUS can handle this situation, difficulties were encountered. The nature and extent of these difficulties were not pursued and consequently FX2-VENUS was not employed in any of the comparisons presented in the RESULTS section of this report.

All of the other three analytical methods proved capable of calculating the specified cases at least up to the point of significant mesh distortion or final neutronic shutdown. A review of the basic calculational techniques employed and significant differences among the three codes follows.

A. FX2-POOL

This analytical tool presents a coupling to the FX2 and POOL computer codes.[2,3,4] Both of these programs utilize two-dimensional cylindrical (R-Z) geometry and have fixed spatial (Eulerian) grids.

The neutronics are supplied by FX2 which is a space-dependent kinetics treatment based on diffusion theory. Reactivity

feedback due to both Doppler broadening of the cross sections and displacement (material motion) is treated explicitly. Based on material and temperature-dependent nine-group cross-section sets, which are prepared a priori, FX2 calculates temperature-adjusted cross sections for each mesh cell. Explicit k-calculations are then performed for determining changes in the state of criticality due to temperature and material motion effects. If there are multiple hydrodynamic time steps per FX2 k-calculation then a quadratic time extrapolation provides the reactivity feedback at each time step.

Thermodynamics and Eulerian hydrodynamics are modeled with POOL, which was developed specifically to analyze boiling pools of fuel and steel. Although this code is capable of treating fuel-steel heat transfer and buoyancy effects, these options were not used.

A limitation on the use of FX2-POOL in this comparison study is:

- The initial delayed neutron precursor concentration must correspond to steady-state conditions at the specified initial power level for the disassembly calculation.

During the analysis of the results presented herein a rather subtle but significant difference between FX2-POOL and PAD/VENUS-II surfaced. PAD and VENUS-II require as input the prompt neutron lifetime whereas FX2 generates its own. This fact was not recognized when specifying the reactor model, but upon examining of power and reactivity histories it became apparent that there was an inconsistency which a prompt neutron lifetime

discrepancy could, and did, explain.

Another, substantially less significant, inconsistency in the problem specification arose from the fact that FX2-POOL does not accept an input power distribution but uses that resulting from the FX2 k-calculation. The input power profile for VENUS-II was obtained from earlier criticality calculations for the intact core model (containing control elements and sodium). Therefore power distributions were slightly inconsistent between these two codes.

B. PAD

This is a coupled neutronics-hydrodynamics program which evolved from computer models developed to analyze weapons explosions, burst reactor (Godiva) transients, and later the KIWI-TNT reactor destruct experiment. Three one-dimensional geometries (spherical, radial expansion of a cylinder, axial expansion of a cylinder) are available, and the calculation is performed on a Lagrangian grid.

Doppler reactivity feedback is accounted for by a simple equation of the form:

$$C = T^n dk/dT \quad ,$$

where C is the Doppler constant (e.g. - 0.004). This equation is evaluated at each time step for each mass point. Thus the Doppler feedback is mass point weighted as in FX2-POOL, but not weighted spatially according to a neutron importance function.

Energy deposition and displacement reactivity feedback are provided in a manner similar to FX2-POOL, with the state of criticality, fluxes, powers, etc., being determined by explicit DTF

transport calculations. A quadratic time extrapolation between the DTF calculations provides the displacement feedback at each hydrodynamic time step.

C. VENUS-II

This is a coupled neutronics-hydrodynamics code developed to analyze postulated LMFBR disassembly accidents.[5,6] Like FX2-POOL, it utilizes two-dimensional R-Z gemoetry, but with Lagrangian hydrodynamics.

Doppler reactivity feedback is calculated via an equation similar to that in the PAD code. The difference is that the change in reactivity due to temperature rise is calculated for zone (mass) averaged temperatures with a weighting coefficient input to each core zone. For the reactor model described in the following section, these weighting factors were 0.55 and 0.45 for the inner and outer core zones, respectively.

Reactivity changes due to material motion are calculated from an input tabulation of spatially dependent reactivity worths. Both reactivity worths and spatial power distributions must be predetermined, i.e., by an R-Z diffusion theory or transport theory calculation.

As previously mentioned this latter point is in contrast to both FX2-POOL and PAD which generate their own flux and power profiles via explicit k-calculations. Thus both prompt neutron lifetime and power profile differences were present during these initial calculations.

In future calculations involving these three codes, neutron

lifetime differences can be avoided by using the FX2 determined value as input to both PAD and VENUS-II. Power profile differences between FX2 and VENUS-II can similarly be removed. Due to the one-dimensional geometry in PAD it is not possible to model exactly a two-dimensional power profile. However, hydrodynamic and neutronic material densities are separable in PAD and thus the power profile can, if desired, be adjusted to any shape. In particular the PAD calculations in this study had a radial (spherical) power density which matched that radial (cylindrical) power density input into the VENUS-II runs.

D. Equation-of-State-(EOS) Modeling

As with the neutronic and hydrodynamic modeling in these three codes, the thermodynamic models also differ. Given the correctness of the basic hydrodynamic fluid description of the reactor, then the EOS model is probably the least well-founded of all the physical models in these disassembly codes. It is important that these be put in perspective.

For LMFBR voided core disassembly analyses such as considered in this study, the energy releases are governed almost entirely by Doppler reactivity feedback. Final neutronic shutdown is provided by material motion which in turn is substantially dependent on the EOS model. However, at the time of significant displacement reactivity feedback the energy deposition is by and large complete.

Another feature of the voided core disassemblies considered is that due to the Doppler reactivity feedback, peak temperatures are not sufficient to cause the fuel to expand, fill all void space,

and then exert condensed state pressures. Based solely on the coefficient of thermal expansion of molten UO_2 near the melting point, the temperature rise needed to expand and fill the space normally occupied by sodium would be ~13 000 K. Thus for all cases, except possibly those academic cases which had no doppler feedback, hydrodynamic disassembly follows from fuel vapor pressure entirely.

The two areas of the EOS models which then are significant for these calculations are the energy partition and fuel vapor pressure formulations. The latter will be examined first.

1. Fuel Vapor Pressure

Both the FX2-POOL and VENUS-II calculations employed the fuel vapor pressure equation associated with the ANL EOS:[5]

$$P_v(\text{dynes/cm}^2) = \exp(69.979 - \frac{76800}{T} - 4.34 \ell nT).$$

The UO_2 vapor pressure equation which has been used in the PAD code for many years is

$$P_v(\text{atm}) = \exp(14.77 - \frac{53864}{T}) \quad .$$

These two equations are shown in Fig. 1.

2. Energy Partition

Below the melting point of the fuel, the models are essentially identical in all three codes, the energy going into sensible heat according to the general formula

$$\Delta E = C_p(\bar{T})\ \Delta T \quad .$$

At the melt temperature PAD and VENUS-II both have heat sink capabilities to account for the heat of fusion. FX2-POOL

currently does not have this feature, and therefore heat of fusion is not acccunted for.

Above the melting point FX2-POOL and PAD account for the heat of vaporization in similar fashions. VENUS-II analyses were performed with the ANL EOS.[5] The energy-temperature relationship in the latter is based on the principle of corresponding states and does not explicitly account for the heat of vaporization. However, it should be emphasized that this EOS was developed and formulated for applications in the range of fuel energy densities for which heat of vaporization effects are not substantial.[7]

Thus, aside from the ANL EOS being different in formalism beyond the melting point, it would be expected that VENUS-II, relative to FX2-POOL and PAD, would overpredict the fuel temperature, the magnitude of the overprediction increasing with increasing fuel energy density up to the point of complete vaporization in a cell. An estimate of the temperature rise equivalent of the heat of vaporization is

$$\Delta T_{eq} \approx \frac{L}{C_p} \approx 4000 \text{ K} ,$$

where approximate values for the heat of vaporization, L, and heat capacity, C_p, are 2000 J/g and 0.5 J/g-K, respectively. However, considering the basically different energy partition formulations in these codes and the (generally) small mass of fuel vaporized prior to substantial material expansion, this temperature rise equivalent of the heat of vaporization should only be considered as indicative of the trend to be expected in the calculated temperatures when intercomparing results.

III. MODEL SPECIFICATIONS

In deciding upon a physical model, arguments in favor of simple, highly idealized specifications must be weighed against those favoring a more complex geometric/material model. The former would permit a cleaner comparison while the latter would relate more closely to accident scenarios which, although extremely unlikely, have been delineated.

Since these two considerations are not optimized for the same model specifications, the approach taken in defining the system to be calculated was to start from the more complex situation and then simplify it as much as seemed reasonable. For example, since analytical and experimental studies indicate that heat transfer is not an important factor in severe disassembly accidents, it was decided that heat transfer options (available only in FX2-POOL and PAD) would not be used.

The reactor model decided upon is similar to an earlier 2100-liter LMFBR design developed by General Electric. Additionally it was specified that the geometry and material distribution correspond to the intact reactor, void of sodium in all regions. Most physical and neutronic specifications for this system are given in the Appendix. A few features not detailed in the Appendix but agreed upon for these comparison calculations are:

- Core BeO and control material is considered as steel, i.e., core steel volume fraction = 0.237 + 0.048 = 0.285.
- No regions will be permitted to support tension, i.e., structural strength ≡0.

- Initial fuel and steel theoretical densities are 9.95 and 7.9 g/cm^3, respectively.
- Fuel heat capacity = 0.548 J/g-K, for all temperatures. Note that this was an oversight in that FX2-POOL and VENUS-II both used the ANL EOS value of 0.437, about 20% less.
- Any other fuel properties which may be needed are to correspond to UO_2, not mixed oxide.
- Delayed neutron precursor concentrations reflect equilibrium conditions at normal operating power, 840 MW.
- Initial core fuel temperatures are proportional to the power distribution.
- Initial reflector (blanket) temperatures are constant at 1000 K.
- No fuel-steel heat transfer.

Two sets of initial conditions (reactivity, power, temperature) were agreed upon. The first, case A, is a scale up (to 2100 ℓ) from a SAS flow coastdown analysis for the FTR. Case B represents a nominal power fiducial.

	Case A	Case B
Reactivity, $	1.05	1.00
Power, MW	1.7+06	1000
Av Core Temperature, K	2500	1500

In order to enable comparisons, including the FX2-POOL code, variants of cases A and B were also run. As described in the previous chapter, FX2-POOL currently requires that initial delayed neutron precursor concentrations correspond to equilibrium conditions at the specified initial power level of the reactor. Moreover, although FX2-POOL will accept any initial temperature distribution, like PAD it has no algorithm (such as VENUS-II has) for having the initial temperatures calculated internally for a specified core average value and a base temperature. Thus for simplicity, those comparison calculations involving FX2-POOL had a flat (spatially independent) initial temperature profile. Additionally, it was decided to run one other variant of these base cases, namely calculations with zero Doppler feedback. These latter analyses were made only to remove a variable in the comparisons and observe the change in agreement, if any, relative to the normal Doppler cases.

For clarity, a summary of the base cases and variations thereof is presented in Table I, followed by an intercomparison of these cases in the sequence listed in this table.

A-1: PAD and VENUS-II

This is the nominal base case A. Differences between the two analyses include:

- Doppler treatment
- UO_2 EOS

- Geometry, 1-Dimensional spherical vs 2-Dimensional cylindrical
- Power and temperature profiles, this results directly from geometric differences.

A-2: PAD and VENUS-II

This is identical to case A1 with the one exception:

- Doppler = 0.0.

TABLE I

OVERVIEW OF COMPARISON CASES

Case Identification	Code	Doppler Constant	Initial Temp Distribution
A1	PAD VENUS-II	-0.004	Spatially dependent
A2	PAD VENUS-II	0.0	Spatially dependent
A3	FX2-POOL PAD VENUS-II	-0.004	Flat
A4	PAD	-0.004	Spatially dependent
B1	PAD VENUS-II	-0.004	Spatially dependent
B2	PAD VENUS-II	0.0	Spatially dependent
B3	FX2-POOL PAD VENUS-II	-0.004	Flat
B4	VENUS-II	-0.004	Spatially dependent

This variation of case A1 was made only to remove a variable from the comparison and to observe the change in agreement, if any.

A-3: FX2-POOL, PAD, and VENUS-II

In order to facilitate intercomparisons, including the FX2-POOL code, the following two departures were made from case A1:

- Flat initial core temperature distribution i.e., all UO_2 temperatures = 2500 K.
- Initial delayed neutron precursor concentration corresponded to steady state at the initial power level, 1.7×10^6 MW.

A-4: PAD

This case was run after the initial analyses uncovered the heat capacity discrepancy. All input specifications are identical to the PAD A-1 run except heat capacity. For this case only the heat capacity was set equal to 0.437J/g-K, the value used in all FX2-POOL and VENUS-II calculations.

B-1: PAD and VENUS-II

This is the nominal base case B. Differences between the two analyses are the same as those listed for case A1.

B-2: PAD and VENUS-II

This is identical to case B1 with the one exception:

- Doppler = 0.0 .

B-3: FX2-POOL, PAD, and VENUS-II

As with cases A1 and A3, the following two differences exist

between B1 and B3:

- Flat initial core temperature distribution i.e., all UO_2 temperatures = 1500 K.
- Initial delayed neutron precursor concentration corresponded to steady state at the initial power level, 1000 MW.

B-4: VENUS-II

This is identical to the Venus-II analysis of case B1 with one exception:

- The initial temperature profile was flatter than that employed in case B1 due to a higher base temperature specification.

Although the initial temperature profile in this case was not judged to be as realistic for this case, the results are presented since they indicate the effect of this input specification on the fission energy release.

In mapping the specified R-Z reactor geometry onto the PAD spherical grid, masses and densities were conserved. Experience with PAD in calculating various severe reactor transient experiments (which had clearly nonspherical geometries) has shown that this is a more accurate approach in general than, for example, to conserve a characteristic dimension. The equivalent spherical radii employed in the PAD calculations were thus:

Core Zone I o.d. = 124.26 cm

Core Zone II o.d. = 158.88 cm

Reflector thickness = 10.56 cm .

The reflector material had the radial blanket composition listed in the Appendix. The thickness was chosen to give the desired radial core power profile.

IV. RESULTS

The significant outputs from these disassembly calculations which are reported and compared are:

- fission energy
- energy in molten fuel
- kinetic energy/work
- power
- reactivity
- pressures and temperatures .

For all cases the energies and system maxima (power, reciprocal period (α), temperature) are listed in Table II. Examination of this table leads to the following significant observations:

- The one comparison which was made with consistent heat capacities, A-1 (VENUS-II) vs A-4 (PAD), showed excellent agreement in the fission energy deposition, $\sim$0.5% difference.
- For all other PAD/VENUS-II comparisons there existed the heat capacity discrepancy. As indicated by the two PAD runs, A-1 and A-4, and the sensitivity studies described in Ref. 6, the fission energy varies linearly with heat capacity for voided core disassembly calculations. It is then estimated that using the same heat capacity would bring the PAD/VENUS-II agreement in fission energy release.

TABLE II

ENERGY RELEASES AND SYSTEM MAXIMA

Case I.D.	Code	Initial Fuel Temperature, K Peak	Initial Fuel Temperature, K Av	Doppler Constant	Fission Energy MJ	Molten Fuel Energy MJ	Kinetic Energy MJ	Maximum Power MW	Maximum α s^{-1}	Maximum Temperature K
A1	PAD	3 040	2 500	- 0.004	5 120	3 210	14.5[a]	1.83 +6	262	4 760
	VENUS-II	3 230	2 500	- 0.004	4 380	3 080	80.6	1.76 +6	262	5 620
A2	PAD	3 040	2 500	0.0	14 600	12 700	NA	1.01 +7	1 100	6 740
	VENUS-II	3 230	2 500	0.0	11 770	10 500	NA	8.90 +6	NA	9 525
A3	FX2-POOL	2 500	2 500	- 0.004	10 190	NA	NA	7.62 +6	262	6 350
	PAD	2 500	2 500	- 0.004	12 400	10 500	NA	7.51 +6	262	5 780
	VENUS-II	2 500	2 500	- 0.004	10 200	NA	NA	6.60 +6	262	7 260
A4	PAD	3 040	2 500	- 0.004	4 400	2 700	9.9	1.80 +6	262	4 750
B1	PAD	2 100	1 500	- 0.004	7 860	2 430	8.0[b]	2.85 +6	1 700	4 370
	VENUS-II	2 230	1 500	- 0.004	6 300	2 390	35.2	2.12 +6	1 670	5 000
B2	PAD	2 100	1 500	0.0	24 700	19 270	NA	4.64 +7	3 050	7 680
	VENUS-II	2 230	1 500	0.0	25 000	24 000	NA	4.74 +7	NA	21 300
B3	FX2-POOL	1 500	1 500	- 0.004	11 770	NA	NA	3.77 +6	2 170	5 700
	PAD	1 500	1 500	- 0.004	10 570	5 140	16.1[c]	2.82 +6	1 700	4 770
	VENUS-II	1 500	1 500	- 0.004	9 500	NA	NA	2.00 +6	2 180	5 990
B4	VENUS-II	1 750	1 500	- 0.004	7 970	3 760	NA	2.03 +6	1 690	5 400

NA = Not Available.

Core averaged fuel vapor pressure (at $V/V_o = 8$).
a = 5.2 atm; b = 3.1 atm; c = 6.4 atm.

within ∿ ± 5% for all cases except B2.

- For cases A3 and B3 the FX2-POOL fission energies are in reasonable agreement with both the VENUS-II and PAD results. This is in spite of the FX2-POOL model inadvertently using only one core enrichment zone and the very different Doppler treatments.
- VENUS-II fission energies as calculated by P. Abramson at ANL and J. Boudreau at LASL (case B3) were identical. In addition, for an entirely different VENUS-II problem, the same input deck when run at ANL, BYU, and LASL has yielded identical results to within the roundoff and significant figure capabilities of the computers.[7]
- Calculated kinetic energies are much less than the fission energies. Furthermore, in spite of the fact that PAD calculates kinetic energy (which was evaluated at a system volume expansion of 8) and VENUS-II calculates the work potential (evaluated via a cell by cell isentropic expansion to 1 atmosphere) the difference between these quantities is still not large.
- Two cases, A2 and B2, had zero Doppler feedback. Although relative agreement between PAD and VENUS-II fission energies was essentially the same as for all other cases, this may be simply the result of replacing one neutronic shutdown effect (Doppler) for another (displacement) when both effects are modeled differently in both codes.

It should be emphasized that calculations (A2 and B2) are purely academic and were run only to accentuate possible displacement feedback and/or high-energy density effects. Obviously the former were similar (due to the relatively good agreement in total energy release). However, as brought out dramatically by the peak temperatures, the energy partition models in PAD and VENUS-II diverge considerably at these extreme energy densities. These zero Doppler comparisons accentuate the need to better understand the accuracy and range of applicability of the energy partition models in these codes.

In the following few pages the four cases A1, A3, B1, and B3 will be examined in some detail and in the above order.

A-1: PAD and VENUS-II

The power and net reactivity histories are shown in Figs. 2 and 3, respectively. The slight differences between the pairs of curves may be explained by examination of Figs. 4 and 5, the Doppler and displacement reactivity traces. Doppler feedback is initially stronger with VENUS-II. This is probably attributable to the higher temperatures calculated by VENUS-II for the same energy deposition, which in turn results from the lower heat capacity and energy partition model effects. This results in a somewhat lower peak power. It is interesting to note that at about that time when all core regions have gone through the melt transition (~1.5 ms) the calculated Doppler reactivities are nearly identical.

The power spike is turned over entirely by Doppler feedback; however, neutronic shutdown results from the strong displacement

reactivity feedback. This is similar for both codes up to about 3.5 ms, at which time VENUS-II shows a much steeper reactivity decrease. This is probably due to a combination of the higher peak fuel vapor pressures as well as geometric effects. This strong departure does not affect the total energy release by more than a few percent due to the already reduced power level at the time of this divergence. Due to the dominance of Doppler feedback for all realistic cases, the differing geometric feedbacks have little influence on the results.

Peak (core center) fuel temperatures and vapor pressures vs time are shown in Figs. 6 and 7. The large divergence is due to a combination of energy partition model differences and peak-to-average power profile differences in the one- and two-dimensional geometries. Perhaps most significant is the result that in spite of relatively large differences in peak temperatures and vapor pressures, core averaged properties, particularly Doppler feedback, are in good agreement. Thus global characterization of this contrived, severe disassembly accident is afforded by both codes.

A-3: FX2-POOL, PAD, and VENUS-II

Power and reactivity histories are shown for this case in Figs. 8 and 9, respectively. The PAD-VENUS-II agreement is noticeably good. The initial agreement among all three codes is very satisfactory; however, due to a model limitation in FX2-POOL and the initial specifications for this case, the net reactivity trace diverges from that of PAD and VENUS-II at about 0.4 ms. Recall that (1) case A3 has a flat initial fuel temperature distribution and (2) FX2-POOL does not account for heat of fusion. The flattening of the net reactivity history between 0.4 and 0.8 ms results from

the nearly zero Doppler feedback as large core regions remain at the melt temperature for a few tenths of milliseconds. Although not explicitly shown on Fig. 9, displacement feedback remains nearly zero until ∿1.6 ms at which time it increases very quickly and controls the neutronic shutdown.

B-1: PAD and VENUS-II

Figures 10 and 11 show the power and net reactivity histories for this case. As with case A1, these curves are most easily interpreted by examination of Figs. 12 and 13, which show the Doppler and displacement feedback reactivities as functions of time. Once again, the initial VENUS-II Doppler feedback is slightly larger than that calculated by PAD. The explanation is identical to that discussed under case A1. Once again the higher temperatures calculated by VENUS-II result in a somewhat lower peak power.

The individual and net reactivity feedback traces are very similar up about 7 ms. At this time the Doppler feedback is diminishing due to the reduced power level, and the input reactivity ramp is causing the net reactivity to flatten or turn up slightly for about 2 or 3 ms. At this time the displacement reactivity feedback begins to predominate and leads to neutronic shutdown.

The slight positive displacement feedback calculated by PAD which peaks around 7 ms (at a value of 0.02 dollars) results from the initial, inward motion of the interface between the two core zones. This effect is also present in the VENUS-II analysis; however, the positive radial feedback is less than the negative axial feedback, with the net displacement reactivity being monotonic. As with Case A1, the VENUS-II displacement reactivity eventually

exhibits a much stronger time dependence than that of PAD. However, this occurs when the power excursion is essentially complete and thus it does not influence the total energy release.

Core center fuel temperature and vapor pressure histories are shown in Figs. 14 and 15. The divergence in these peak values was also noted in case A1 and qualitatively the explanation is the same. However, system-averaged properties agreed well and thus global characterization of this contrived, severe disassembly accident is also afforded by both codes.

B-3: FX2-POOL, PAD, and VENUS-II

This case affords a relatively clean comparison among the three calculational methods; thus it was decided to examine the power, reactivity, and temperature histories more closely and quantitatively. The power traces are shown in Figs. 16 and 17 and the reactivity traces in Fig. 18. It was expected that the initial power rise (until feedback effects become significant) would be very similar for all three codes. After significant temperatures and pressures were generated some departures in the power and reactivity curves were to be expected since Doppler and displacement reactivity feedbacks (among other effects) are modeled differently in all three codes.

It appears that the PAD and VENUS-II power and reactivity curves are internally consistent, at least up to the time of peak power for the first power spike. A very small difference in the delayed neutron fraction ($\sim$5%) between these two codes results in the PAD absolute reactivity (not in dollars) being slightly larger than that of VENUS-II through the first few milliseconds. This qualitatively

explains even the relatively minor PAD and VENUS-II power profile differences for these early times. The apparent anomaly between FX2-POOL and the other two codes during the first few milliseconds has the following explanation.

Although the specifications for the kinetics parameters, delayed neutron fraction, and neutron lifetime are listed in Appendix A, FX2 calculates and uses its own prompt neutron lifetime and employs a slightly different delayed neutron fraction. VENUS-II and PAD, on the other hand, require as input the neutron lifetime. Thus, differences in this basic parameter could explain the initial power divergence of FX2-POOL. Upon investigation of the prompt neutron lifetime calculated by FX2, the value of 0.401 ms was uncovered. This lower lifetime is sufficient to explain the peak power anomaly.

In order to quantify the explanation one can, to first order, neglect delayed neutrons and from the point kinetics equation arrive at the relationship

$$\frac{\hat{n}_{FX2}}{\hat{n}_{\substack{PAD\ or \\ VENUS\text{-}II}}} = \exp\left[\int_{t_1}^{t_2}{}_{FX2}\ \alpha(t)\,dt - \int_{t_1}^{t_2}{}_{\substack{PAD\ or \\ VENUS\text{-}II}}\ \alpha(t)\,dt\right],$$

where $\hat{n}$ = peak neutron density or power

α = $\Delta k/\ell$ = prompt reciprocal period

t_1 = 0 for this case, and

t_2 = the time of peak power, i.e., when system reactivity passes through zero.

A hand evaluation of the areas under the reactivity curves in Fig. 18 and using the specified prompt neutron lifetime of 0.6

ms result in peak power ratios in gross disagreement with those obtained from Fig. 17. However, using these same integrated reactivities, but lifetimes of 0.401 and 0.6 ms, respectively, for FX2-POOL and either PAD or VENUS-II, results in predicted peak power ratios in satisfactory agreement with those from Fig. 17.

Temperature Discrepancy

One result which is under investigation is differences in peak (core center) temperature. Consider, for example, the peak temperatures and total fission energies of case B3, repeated here for clarity.

	FISSION ENERGY (MJ)	PEAK TEMPERATURE (K)
FX2-POOL	11 770	5700
PAD	10 570	4770
VENUS-II	9 500	5990

Recall that FX2-POOL does not account for heat of fusion and its calculational model inadvertently had only one core enrichment zone. Both of these differences, relative to VENUS-II and PAD, would tend toward higher peak temperatures for FX2-POOL. Another point is that FX2 calculates its own power distribution and VENUS-II and PAD employed an input distribution from a prior k-calculation. This latter effect should be very minor.

Heat of vaporization effects (which the VENUS-II calculations did not account for) act in the opposite direction; they would tend toward higher peak temperatures for VENUS-II. These individual effects will be eliminated where possible in future comparisons and otherwise quantified in order to enable a more precise and complete understanding of the calculated temperatures.

Finally, consider case B2 which was run only to emphasize the different displacement feedback models used in PAD and VENUS-II. (Recall that for all cases except A2 and B2, Doppler feedback and not displacement feedback was the dominant factor in determining the total energy release.) The total energies and peak temperatures for this case are listed below:

	FISSION ENERGY (MJ)	PEAK TEMPERATURE (K)
PAD	24 700	7680
VENUS-II	25 000	21 300

Obviously there are significant model differences in the two codes when they are applied to extreme situations such as these. An attempt is being made to understand these calculated temperatures.

V. PRELIMINARY CONCLUSIONS

Due to the (generally slight) inconsistencies in physical data and in the geometric and material models present in these initial comparison calculations, any conclusions should be considered tentative. With this caveat, then, the significant conclusions follow directely from the reasons why this study was felt to be worthwhile, as stated in the Introduction.

- All three calculational methods are internally consistent in predicting the total energy deposited in the fuel, at least for the models and other specified conditions employed herein.
- For similar total energy depositions, calculated (peak) temperatures diverge rather strongly, the divergence increasing monotonically with fuel internal energy. This is

due to the inherently different energy-temperature relationships in the codes. It appears that heat of vaporization effects may largely account for these differences, which are currently being investigated.

- Kinetic energy and work potential, which are measures of the damage potential of an excursion, are orders of magnitude less than the fission energy.

VI. FUTURE EFFORTS

Prior to analyzing the results presented herein it was planned to perform comparison calculations for some of these same cases but at input reactivity insertion rates of 20 and 200$/s. These calculations will still be made and should provide useful information relative to the range of applicability of these three computational methods. First, however, an attempt will be made to better and more completely document and understand at least one case, e.g., B3. Here particular reference is made to fuel temperatures as calculated by the different codes.

REFERENCES

1. W. R. Stratton, L. B. Engle, and D. M. Peterson, "Reactor Power Transient Studies," International Conference on Engineering of Fast Reactors for Safe and Reliable Operation, Karlsruhe, Germany, Oct. 9-13, 1972.

2. D. A. Meneley, G. K. Leaf, A. J. Lindeman, T. A. Daly, and W. T. Sha, "A Kinetics Model for Fast Neutron Analysis in Two Dimensions," Symp. on Dynamics of Nuclear Systems, Tucson, Arizona, Nov. 23-25, 1970.

3. W. T. Sha, T. A. Daly et al., "Two-Dimensional Fast Reactor Disassembly Analysis with Space Time Kinetics," ANS Topical Meeting on New Developments in Reactor Mathematics and Applications, Idaho Falls, March 24-31, 1971.

4. P. B. Abramson, "POOL-A Two-Dimensional Three-Component Coupled Hydrodynamic Thermodynamic Computer Model for Boiling Pools of Fuel and Steel," Argonne National Laboratory report RSA-TM-3 (May 1975).

5. J. F. Jackson and R. B. Nicholson, "VENUS-II: An LMFBR Disassembly Program," Argonne National Laboratory report ANL-7951 (September 1972).

6. R. B. Nicholson and J. F. Jackson, "A Sensitivity Study for Fast-Reactor Disassembly Calculations," Argonne National Laboratory report ANL-7952 (January 1974).

7. J. F. Jackson, Brigham Young University, personal communication, August 1975.

APPENDIX

With the exception of the cellwise reactivity worths and specific powers which were necessary for the VENUS-II calculations, all other reactor and nuclear data are given below. The former are available, but too cumbersome to be conveniently reported.

1. Reactor Power

Core	840 MW
Axial Blanket	32 "
Radial Blanket	63 "
Total	935 "

2. Core Dimensions (Nominal)

Core Height	76 cm (30 in.)
Core Zone 1 o.d.	130 cm (51 in.)
Core Zone 2 o.d.	185 cm (73 in.)
Axial Blanket Height (upper, lower, each)	38 cm (15 in.)
Radial Blanket Height	152 cm (60 in.)
Radial Blanket Thickness	35 cm (14 in.)
Core Volume	2100 liters

3. Core Average Composition (vol%)

Fuel	30.8
Steel	23.7

Sodium	40.7
BeO & Control	4.8

4. Radial Blanket Composition (vol%)

UO_2 (natural)	49.5
Steel	18.9
Sodium	31.6

5. Nuclear Data

Average Enrichment, % Fissile Pu in Total (Pu + U)	17.2
Fissile Inventory	
Core	969
Axial Blanket	89
Radial Blanket	267
Total	1325 kg
Fuel (core) smear density	90 %
Fuel mass, (U + PU) O_2	6500 kg
Doppler Value (T dk/dT)	
Sodium-in	-0.0060
Sodium-out (blankets & core)	-0.0040

6. Point Kinetics

Neutron lifetime	6.0 E-7 s
Precursor groups	6
Delayed Neutron Fractions	7.9 E-5
	6.87 E-4

(1$ = 3.151 E-3)	5.88 E-4	
	1.135 E-3	
	5.01 E-4	
	1.61 E-4	
Decay constant per precursor group	1.28 E-2	s-1
	3.14 E-2	
	1.35 E-1	
	3.43 E-1	
	1.37	
	3.80	

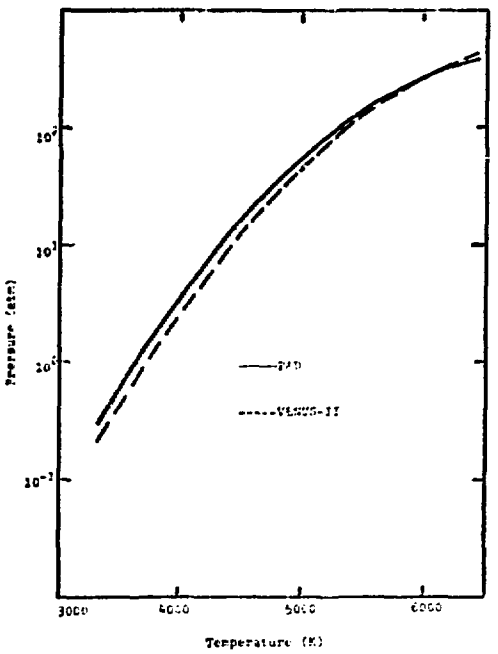

Fig. 1. Saturated UO_2 vapor pressure dependence on temperature.

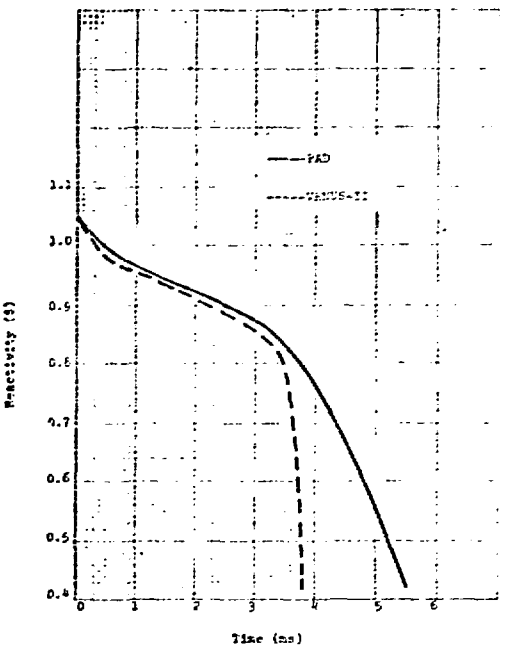

Fig. 3. Net reactivity, case A1.

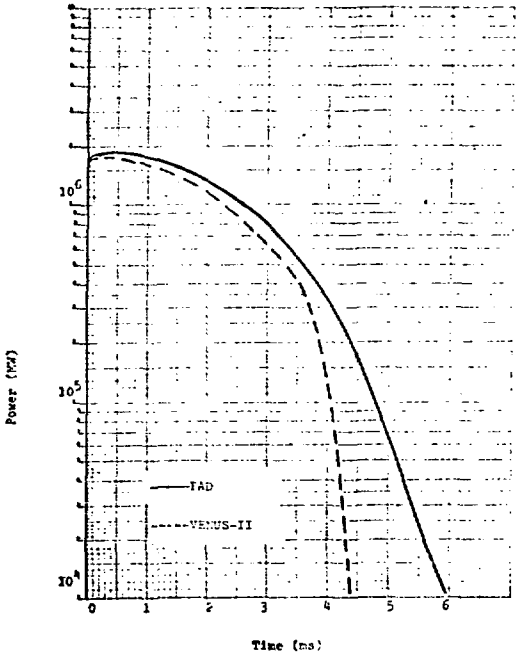

Fig. 2. Power history for case A1.

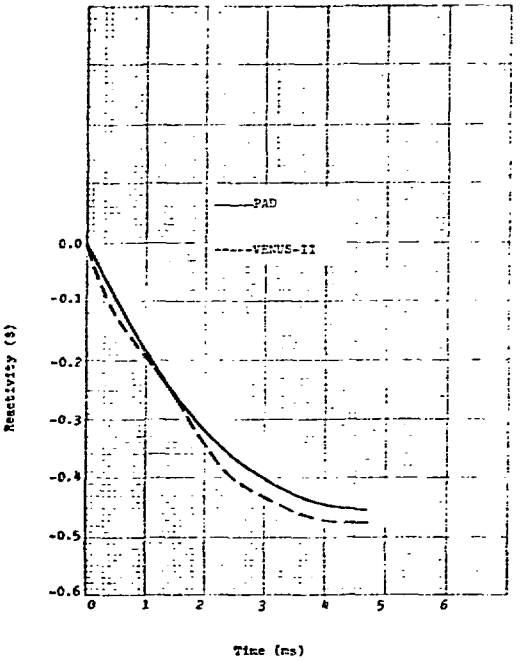

Fig. 4. Doppler reactivity, case A1.

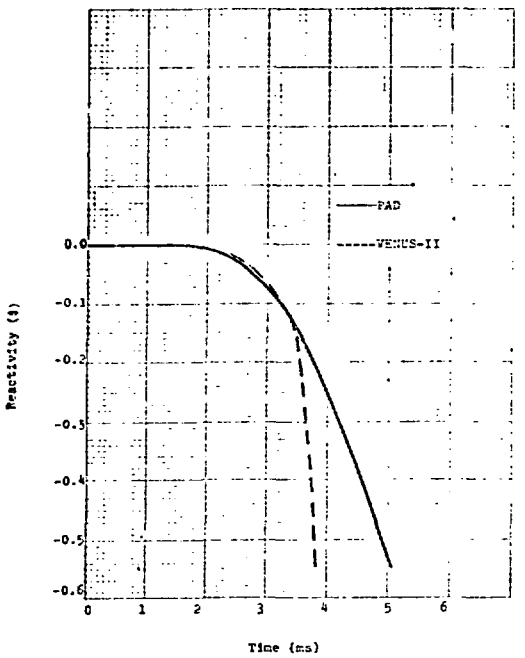

Fig. 5. Displacement reactivity, case A1.

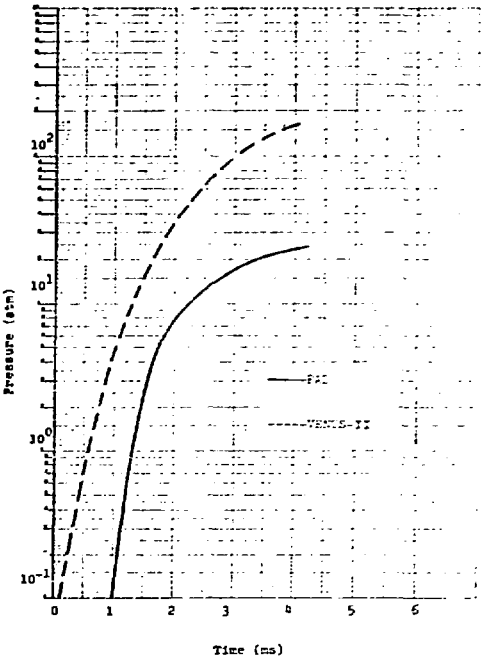

Fig. 7. Core center fuel vapor pressure, case A1.

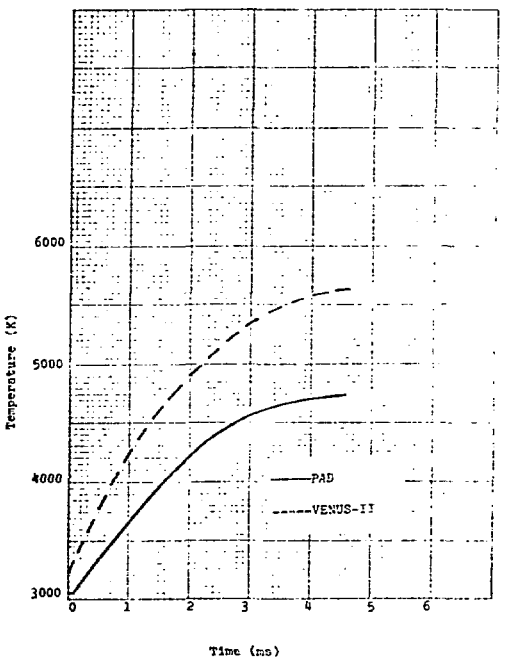

Fig. 6. Core center fuel temperature, case A1.

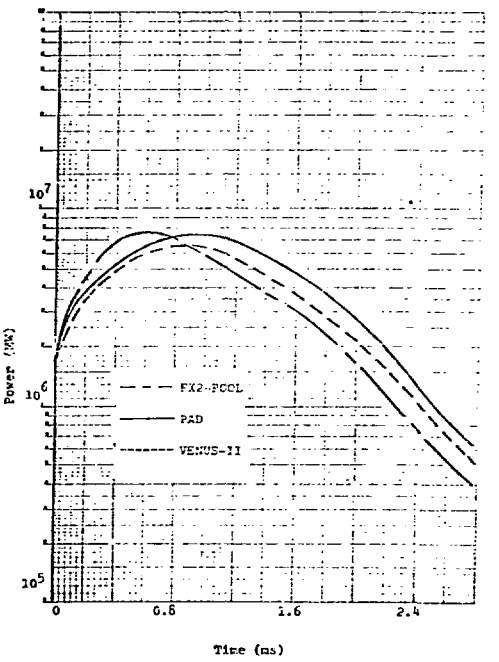

Fig. 8. Power histories, case A3.

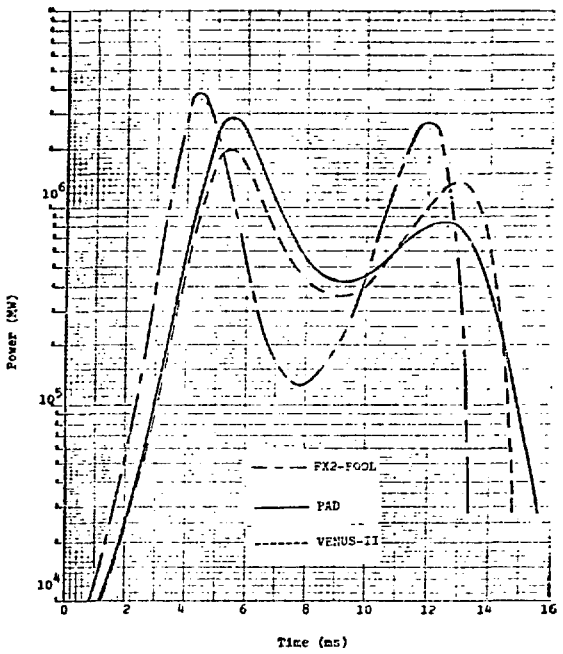

Fig. 17. Power history, case B3.

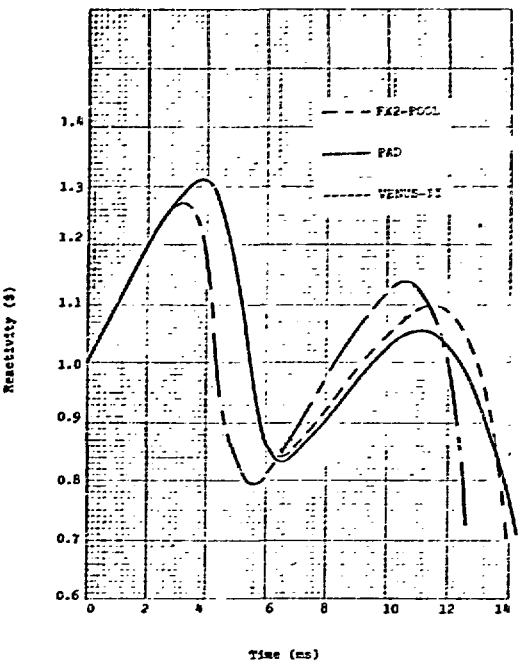

Fig. 18. Net reactivity, case B3.

☆ U.S. GOVERNMENT PRINTING OFFICE: 1975—677-343/52

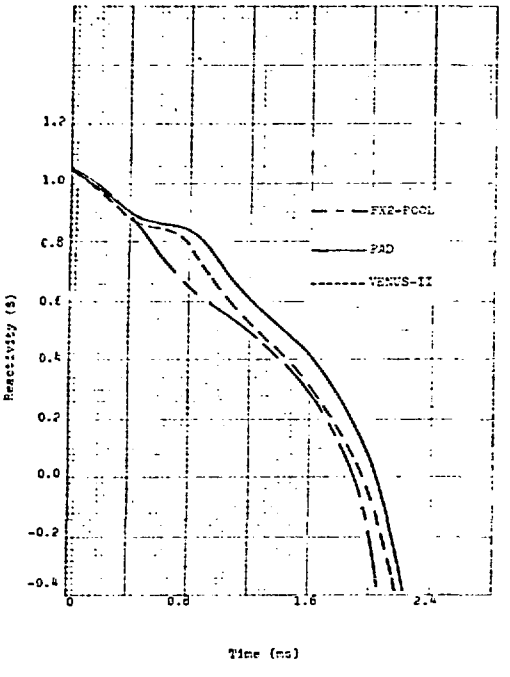

Fig. 9. Net reactivity, case A3.

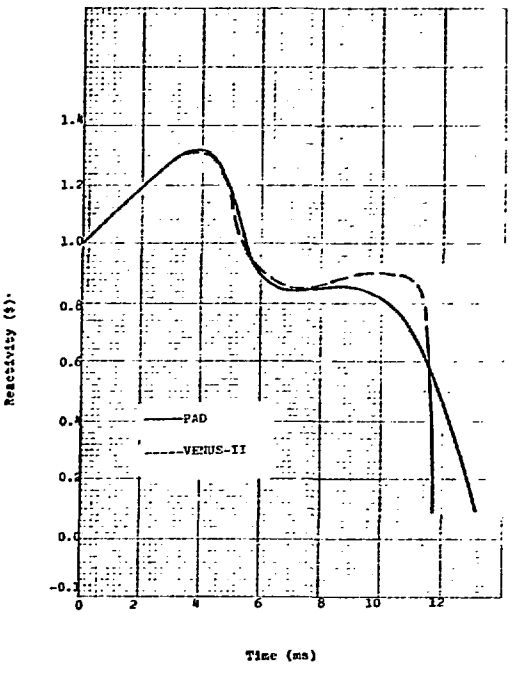

Fig. 11. Net reactivity, case B1.

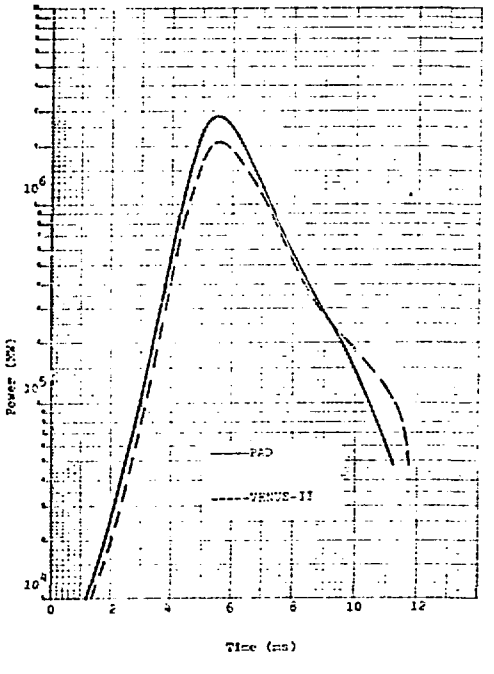

Fig. 10. Power histories, case B1.

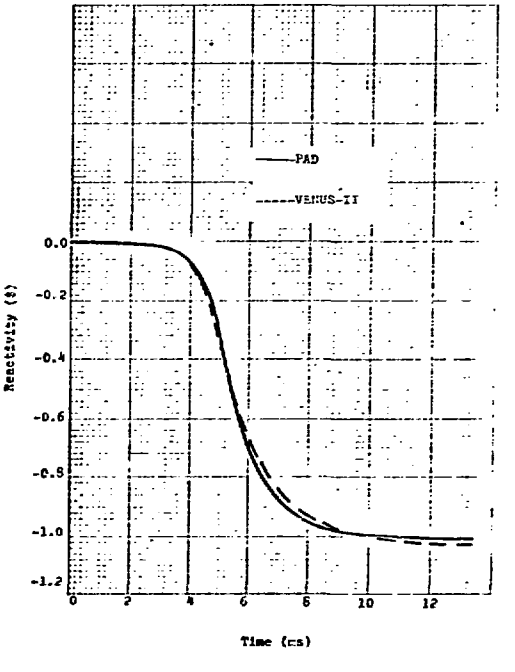

Fig. 12. Doppler reactivity, case B1.

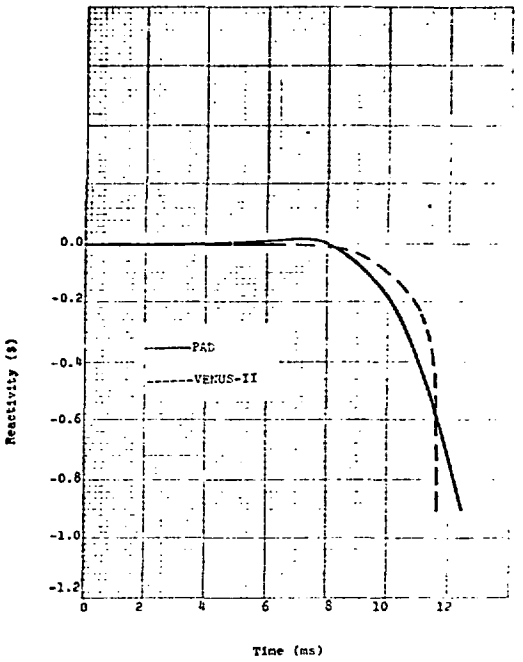

Fig. 13. Displacement reactivity, case B1.

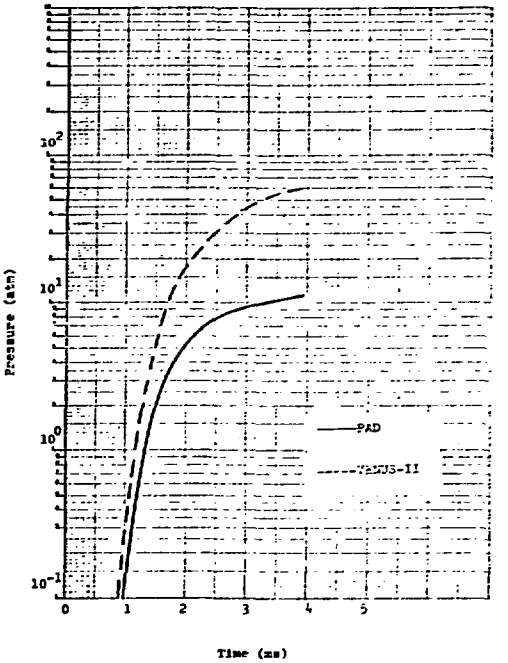

Fig. 15. Core center fuel pressure, case B1.

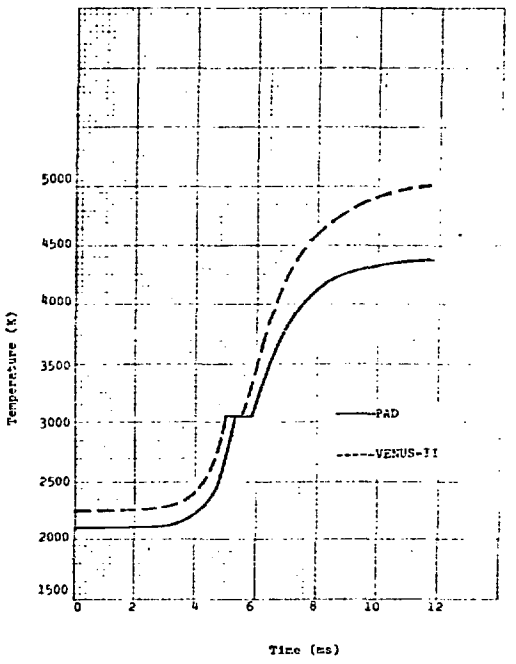

Fig. 14. Core center fuel temperature, case B1.

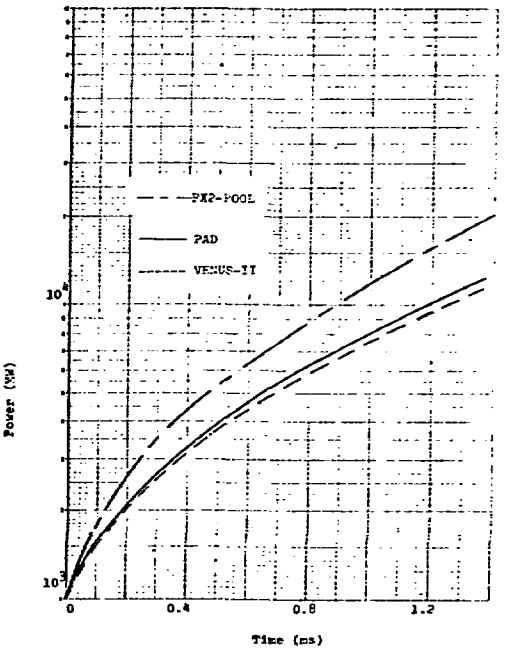

Fig. 16. Power history, case B3.